Fish Physiol Biochem (2012) 38:665–678
DOI 10.1007/s10695-011-9549-1

Effects of low environmental salinity on the cellular profiles and expression of Na^+, K^+-ATPase and Na^+, K^+, $2Cl^-$ cotransporter 1 of branchial mitochondrion-rich cells in the juvenile marine fish *Monodactylus argenteus*

Chao-Kai Kang · Fu-Chen Liu · Wen-Been Chang · Tsung-Han Lee

Received: 9 February 2011 / Accepted: 6 August 2011 / Published online: 24 August 2011
© Springer Science+Business Media B.V. 2011

Abstract The goal of this study was to determine the osmoregulatory ability of a juvenile marine fish, silver moony (*Monodactylus argenteus*), for the purpose of developing a new experimental species for ecophysiological research. In this study, *M. argenteus* was acclimated to freshwater (FW), brackish water (BW), or seawater (SW). The salinity tolerance of this euryhaline species was effective, and the fish survived well upon osmotic challenges. The largest apical surface of mitochondrion-rich cells was found in the FW individuals. Immunohistochemical staining revealed that Na^+, K^+-ATPase immunoreactive (NKA-IR) cells were distributed in the interlamellar region of the gill filaments of the silver moony in all experimental groups. In addition to the filaments, NKA-IR cells were also found in the lamellae of the FW individuals. The number of NKA-IR cells in the gills of the FW individuals exceeded that of the BW and SW individuals. The NKA-IR cells of FW and SW individuals exhibited bigger size than that of BW fish. The NKA activities and protein expression of the NKA α-subunit in the gills of the FW individuals were significantly higher than in the BW and SW groups. Additionally, the relative amounts of Na^+, K^+, $2Cl^-$ cotransporter 1 (NKCC1) were salinity-dependent in the gills. Immunofluorescent signals of NKCC1 were localized to the basolateral membrane of NKA-IR cells in all groups. In the gills of the FW individuals, however, some NKA-IR cells did not exhibit a basolateral NKCC1 signal. In conclusion, the present study illustrated the osmoregulatory mechanisms of this easy- and economic-to-rear marine teleost with euryhaline capacity and proved the silver moony to be a good experimental animal.

Keywords Euryhaline teleost · Gill · Na^+ · K^+-ATPase · Na^+ · K^+ · $2Cl^-$ cotransporter · Osmoregulation · Silver moony

C.-K. Kang · F.-C. Liu · T.-H. Lee (✉)
Department of Life Sciences, National Chung Hsing University, Taichung 402, Taiwan
e-mail: thlee@email.nchu.edu.tw

W.-B. Chang (✉)
National Museum of Marine Biology and Aquarium, 2 Houwan Road, Checheng, Pingtung 944, Taiwan
e-mail: wenbeen@nmmba.gov.tw

W.-B. Chang
Institute of Marine Biodiversity and Evolution, National Dong Hwa University, Hualien 974, Taiwan

Introduction

The silver moony, *Monodactylus argenteus* (Linnaeus 1758), is a marine teleost that is widely distributed in the tropical Indo-West Pacific, including the west coast of Taiwan. The adult fish, which has a silvery appearance and a triangular body shape with rudimentary pelvic fins, is found commonly in estuaries and sometimes in coastal reefs. Juveniles of

this species often occur in estuaries and sometimes in rivers. In addition to their shining appearance, the juvenile fish have two vertical black bands over their head and small ventral fin. These two characters, however, disappear in the adult fish (Shao 2009). The juvenile silver moony has a euryhaline capacity that allows it to survive in environments with different salinities, from freshwater to full strength seawater (Fernhead and Fabian 1971). Because the silver moony is beautiful, euryhaline, easy-to-rear, and inexpensive, it is now a common aquarium species with stable resources in Taiwan.

The gills are organs that are in direct contact with external environments and are major osmoregulatory organs in teleosts. In the branchial epithelium, there are mitochondrion-rich cells (MR cells) known as ionocytes, which are characterized by the presence of a rich population of mitochondria and have osmoregulatory abilities for ion uptake in freshwater (FW) and ion secretion in seawater (SW). The MR cells exhibit polarity, with extensive tubular systems at the basolateral membrane, resulting in a large surface area for ion-transporting proteins to occur, including Na^+, K^+-ATPase (NKA) (Hirose et al. 2003; Evans et al. 2005; Hwang and Lee 2007). Previous studies reported that the apical surfaces of the MR cells in the gills of a number of teleosts changed in size or shape in response to environmental salinity or concentrations of ions (Hossler et al. 1985; Lee et al. 1996; Chang et al. 2002; Katoh and Kaneko 2003; Kaneko et al. 2008).

NKA is a ubiquitous membrane-bound enzyme that couples the exchange of two extracellular K^+ molecules for three intracellular Na^+ molecules via the hydrolysis of one molecule of ATP. In the branchial MR cells, NKA provides a driving force for secondary ion–transporting systems (Marshall and Bryson 1998; Hirose et al. 2003; Hwang and Lee 2007). NKA immunoreactive (NKA-IR) cells were thus thought to present MR cells. Hwang and Lee (2007) reported that euryhaline teleosts usually exhibited the lowest level of branchial NKA expression in environments with salinities similar to their natural habitats. The expression of gill NKA in euryhaline teleosts was species- and salinity-dependent and could be categorized into different patterns, thus providing a driving force for secondary transporter systems in response to changes of environmental salinities.

The Na^+, K^+, $2Cl^-$ cotransporter 1 (NKCC1), which is in the epithelial cells located on the basolateral membrane, plays the role of simultaneously transporting Na^+, K^+, and Cl^- into cells and has been considered to be the secretory isoform (Lytle et al. 1995; Starremans et al. 2003). According to previous review articles, NKCC1 and the cystic fibrosis transmembrane conductance regulator (CFTR) participate in the mechanism underlying Cl^- excretion and represent marker transporters in branchial MR cells of SW teleosts (Marshall 2002; Hirose et al. 2003; Hwang and Lee 2007; Evans 2008). Increased expressions of the NKCC1 gene and protein have been found in the gills of euryhaline teleosts upon salinity challenges. In teleosts, the distribution and expression of branchial NKCC1 protein were detected using a monoclonal anti-human NKCC antibody (T4; Lytle et al. 1995). Immunohistochemical staining of gills with the T4 antibody revealed that NKCC1 is localized to the basolateral membrane of MR cells in SW-acclimated fish (Wu et al. 2003; Hiroi and McCormick 2007; Katoh et al. 2008). However, previous studies using immunohistochemical staining with this antibody in the gills of FW-acclimated euryhaline teleosts revealed three groups: (1) no signal (lake trout, Hiroi and McCormick 2007); (2) immunoreactivity in the apical region of MR cells (killifish, Katoh et al. 2008; sea bass, Lorin-Nebel et al. 2006; tilapia, Wu et al. 2003; Inokuchi et al. 2009; brackish medaka, Kang et al. 2010); and (3) immunoreactive signals localized to the basolateral membrane of MR cells (goby, McCormick et al. 2003; pufferfish, Prodocimo and Freire 2006; sturgeon, Sardella and Kültz 2009). These groups with different immunostaining results indicated that the osmoregulatory mechanisms of the FW-type MR cells varied with fish species. However, the highest levels of immunoreactive signals for NKCC1 were found in hyperosmotic media-acclimated fish.

Lin and Sung (2003) observed the number and distribution of MR cells in *M. argenteus* acclimated to an isosmotic environment (5 g L^{-1}) and to FW. To our knowledge, however, the osmoregulatory mechanisms of this euryhaline species have not been reported to date. As *M. argenteus* has the characteristics of euryhalinity, is easy and economic to rear, and has stable resources available, the goal of the present study was to develop this fish as a new experimental species,

similar to the killifish, *Fundulus heteroclitus*, for ecophysiological studies through illustrating their osmoregulatory ability. The survival rates of individuals transferred from SW to FW or vice versa were observed. Furthermore, silver moony were acclimated to environments of different salinities (FW, BW, SW) for subsequent experiments, including investigation of plasma osmolality, the ultrastructure of the apical surfaces of branchial MR cells, and the expressions of branchial NKA and NKCC1, to compare the osmoregulatory mechanisms among groups.

Materials and methods

Fish and environment

Juvenile silver moony (*Monodactylus argenteus*) with body masses of 3.0 ± 0.5 g and 4.5 ± 0.5 cm total lengths were obtained from a local aquarium. Seawater (35‰; SW) and brackish water (15‰; BW) were prepared from aerated local tap water (freshwater; FW) with proper amounts of synthetic sea salt (Aquarium Systems, Mentor, OH, USA). For experiments, *M. argenteus* were maintained in FW ($[Na^+]$ 0.22 ± 0.01 mM; $[K^+]$ 0.04 ± 0.01 mM; $[Ca^{2+}]$ 0.68 ± 0.01 mM; $[Mg^{2+}]$ 0.28 ± 0.01 mM; $[Cl^-]$ 0.14 ± 0.01 mM), BW ($[Na^+]$ 156.11 ± 4.50 mM; $[K^+]$ 5.72 ± 0.06 mM; $[Ca^{2+}]$ 9.29 ± 0.28 mM; $[Mg^{2+}]$ 30.34 ± 1.29 mM; $[Cl^-]$ 270.60 ± 12.07 mM), or SW ($[Na^+]$ 482.9 7 ± 12.73 mM; $[K^+]$ 11.38 ± 0.07 mM; $[Ca^{2+}]$ 15.34 ± 0.16 mM; $[Mg^{2+}]$ 67.87 ± 1.45 mM; $[Cl^-]$ 572.89 ± 24.24 mM) for at least 4 weeks under 14L:10D at 28 ± 1°C. *M. argenteus* individuals were then analyzed as described below. The water was continuously circulated through fabric-floss filters and partially refreshed every week. Fish were fed a daily diet of commercial pellets.

Salinity tolerance of *M. argenteus* in response to salinity challenge

The two groups of 20 individuals of *M. argenteus* acclimated to FW and SW were transferred directly to SW and FW for 7 days, respectively. The groups were observed, and mortality was recorded every day. When exposed to hyper- and hyposmotic challenges, survival rates of fish indicating the levels of salinity tolerance were determined.

Plasma analyses

Blood was collected from the dorsal artery and vein of the fish with heparinized 1-mL syringes and 27-gauge needles. After centrifugation at 1,000*g* and 4°C for 10 min, the plasma was stored at −80°C until analysis. Plasma osmolality was determined using a Wescor 5520 vapro osmometer (Logan, UT, USA). $[Na^+]$ was determined with a Hitachi Z-8000 polarized Zeeman atomic absorption spectrophotometer (Tokyo, Japan). $[Cl^-]$ was determined using the ferricyanide method (Franson 1985) with a Hitachi U-2001 spectrophotometer. The plasma osmolality and Na^+ and Cl^- concentrations of each fish were calculated as the mean of the replicate samples taken from that fish. Six fish were sampled for each salinity treatment.

Muscle water content

Muscle was sampled from the dorsum of the fish of the FW-, BW-, and SW-acclimated groups, and muscle water content was determined as the percentage of weight loss after drying at 100°C for 3 days.

Scanning electron microscope (SEM)

Excised gills were processed as described in Lee et al. (1996). The gills were fixed at 4°C in a fixative consisting of 5% (v/v) glutaraldehyde and 4% (w/v) paraformaldehyde in 0.1 M phosphate buffer (PB, pH 7.2) for 12 h. Fixed gills were rinsed for 15 min with three changes of 0.1 M phosphate buffer (PB) at 4°C, then post-fixed with 1% (w/v) osmium tetroxide in 0.1 M PB for 1.5 h. After post-fixation, the gills were rinsed in PB and dehydrated in ascending concentrations of ethanol, from 30% to absolute. Samples were then critical point dried using liquid CO_2 in a Hitachi HCP-2 (Tokyo, Japan) critical point drier, mounted on aluminum stubs with silver paint, and sputter coated for 3 min with a gold–palladium complex in a Pt Coater. The coated specimens were observed under a scanning electron microscope (JEOL JSM-6700F, Tokyo, Japan).

Antibodies

The primary antibodies used in this study included: (1) NKA α-subunit: a mouse monoclonal antibody

(α5; Developmental Studies Hybridoma Bank, Iowa City, IA, USA) raised against the α-subunit of avian NKA; (2) NKCC: a mouse monoclonal antibody (T4; Developmental Studies Hybridoma Bank) raised against the human colonic NKCC; and (3) #11: a polyclonal antibody to the NKA α-subunit kindly provided by P. P. Hwang (Institute of Cellular and Organismic Biology, Academia Sinica, Taipei, Taiwan). The secondary antibody used was alkaline phosphate-conjugated goat anti-mouse IgG (Jackson ImmunoResearch Laboratories, West Grove, PA, USA). The secondary antibody used for immunoblots was horseradish peroxidase-conjugated goat anti-mouse IgG (Pierce, Rockford, IL, USA). For double immunofluorescence staining, the secondary antibodies were Alexa Fluor-488-conjugated goat anti-mouse IgG and Alexa Fluor-546-conjugated goat anti-rabbit IgG (Molecular Probes, Eugene, OR, USA).

Paraffin section and immunohistochemical detection of NKA immunoreactive (NKA-IR) cells

The gills all of the fish in the different treatments were excised and fixed in Bouin's solution (Sigma, St. Louis, MO, USA) at room temperature for 48 h. The samples were dehydrated through a graded ethanol series, infiltrated with xylene, and embedded in paraffin. Cross-sections and longitudinal sections of the gills were cut at 7 μm thickness and mounted on poly-L-lysine-coated glass slides. The deparaffinized sections were immunohistochemically stained with a monoclonal antibody (α5) to the NKA α-subunit followed by the use of a commercial kit (PicTure™, Zymed, South San Francisco, CA, USA) for visualization of the immunoreaction. The immunostained sections were then counterstained with hematoxylin (Merck, Hohenbrunn, Germany) and observed under a microscope (Olympus BX50, Tokyo, Japan). Negative control experiments in which PBS was used instead of the primary antibody were conducted (data not shown), to confirm the positive results.

The average values of the cell size and number were determined from 10 filaments of the first and secondary pairs of silver moony gills. For this analysis, samples were randomly selected only from those cross-sections of filaments approximately 175 ± 25 μm in length to minimize the effects of cutting angles on the sections, and micrographs of the sections were taken with a digital camera (Nikon COOLPIX 5000, Tokyo, Japan) for subsequent measurement. The cell size of each filament was obtained from the average size of all NKA-IR cells in that filament quantified by Image-Pro Plus software (Image-Pro Plus version 4.5.0.29, Media Cybernetics). Additionally, the number of NKA-IR cells per filament was counted. These values for different groups of fish were then calculated and compared.

Immunoblotting of NKA (Na^+, K^+-ATPase) and NKCC1 (Na^+, K^+, $2Cl^-$cotransporter 1)

The gill scrapings were suspended in a mixture of homogenization medium (100 mM imidazole–HCl, 5 mM Na_2EDTA, 200 mM sucrose, 0.1% sodium deoxycholate, pH 7.6) with proteinase inhibitors (10 mg antipain, 5 mg leupeptin, and 50 mg benzamidine dissolved in 5 mL aprotinin) (vol/vol: 50/1). Homogenization was performed in microcentrifuge tubes on ice with a Polytron PT1200E (Lucerne, Switzerland) at maximal speed for 15 s. The homogenates were then centrifuged at 13000*g* at 4°C for 20 min. The protein concentrations of the supernatant were determined using reagents from a Protein Assay Kit (Bio-Rad, Hercules, CA, USA), and bovine serum albumin (Sigma) was used as a standard. The prestained protein molecular weight marker was purchased from Fermentas (SM0671; Hanover, MD, USA). Aliquots containing 30 μg of the gill homogenates were heated at 60°C for 30 min and fractionated by electrophoresis on SDS-containing 7.5% polyacrylamide gels. Separated proteins were transferred from the unstained gels to PVDF membranes (Millipore, Bedford, MA, USA) using a tank transfer system (Mini Protean 3, Bio-Rad). Blots were preincubated for 2 h in phosphate-buffered saline with Tween 20 (PBST) buffer (137 mM NaCl, 3 mM KCl, 10 mM Na_2HPO_4, 2 mM KH_2PO_4, 0.2% (vol/vol) Tween 20, pH 7.4) containing 5% (wt/vol) non-fat dried milk to minimize non-specific binding and were then incubated at 4°C with the primary antibody α5 (NKA) diluted in PBST (1: 4000), or T4 (NKCC) diluted in PBST (1:500) overnight. The blots were washed with PBST, followed by a 1-h incubation with AP-conjugated secondary antibody and then developed after incubation with an HRP system (Zymed). The images of the scanned immunoblots

were imported in TIFF format into a commercial software package (MCID software; Imaging Research, Ontario, Canada), and the results were converted to numerical values to compare the relative intensities of immunoreactive bands.

NKA activity

Enzyme activity was measured by the NADH-linked methods (Kang et al. 2008) modified from McCormick (1993). ADP derived from the hydrolysis of ATP by ATPase was enzymatically coupled to the oxidation of reduced NADH using lactate dehydrogenase (LDH) and pyruvate kinase (PK). Two pairs of gills from each fish were dissected quickly and stored in a microcentrifuge tube at −80°C. The tissue was rapidly thawed and homogenized in 650 μL of SEID buffer (150 mM sucrose, 10 mM EDTA, 50 mM imidazole, 0.1% sodium deoxycholate, pH 7.5) containing proteinase inhibitor with a Polytron PT1200E at maximal speed for 10 s on ice. The homogenates were then centrifuged at 5000*g* and 4°C for 2 min. The supernatants were assayed for NKA activity and protein concentration. The assay solution (50 mM imidazole, 0.5 mM ATP, 2 mM phosphoenolpyruvate (PEP), 0.32 mM NADH, 3.3 U LDH mL^{-1}, and 3.6 U PK mL^{-1}, pH 7.5) was mixed with a salt solution (189 mM NaCl, 10.5 mM $MgCl_2$, 42 mM KCl, 50 mM imidazole, pH 7.5) in a 3:1 ratio. Before the assay, a standard curve was determined from 0 to 30 nmol ADP per well at 340 nm at 28°C after adding 200 μL of assay mixture for at least 5 min in a 96-well plate. The slope of the standard curve should be −0.012 to −0.015 absorbance units nmol ADP^{-1}. A 10-μL sample from one fish was loaded into a well, and 200 μL of assay mixture was added with or without 1 mM ouabain; each sample was assayed in triplicate. The plates were read every 15 s for up to 10 min in a VERSAmax microplate reader (Molecular Devices, Sunnyvale, CA, USA) at 340 nm and 28°C. The linear rate from 2 to 10 min for each pair of triplicate wells was determined. The protein concentrations of the samples were determined using Protein Assay Dye (Bio-Rad) with bovine serum albumin (BSA; Sigma) as a standard. The NKA activity was calculated as the difference in the slope of ATP hydrolysis (NADH reduction) in the presence and absence of ouabain and was expressed as μmol ADP per mg protein per hour.

Cryosection and immunofluorescent double staining

Gills from FW-, BW-, and SW-acclimated silver moony were excised and fixed immediately in a mixture of methanol and DMSO (v/v: 4/1) at −20°C for 3 h for double immunofluorescence staining. The tissues were washed with PBS and then infiltrated with O.C.T. (optimal cutting temperature) compound (Sakura, Tissue-Tek, Torrance, CA, USA) overnight at 4°C. The samples were then mounted in O.C.T. compound for cryosectioning. Cross-sections of gills were cut at a 7 μm thickness using a Cryostat Microtome (Microm HM 505E, Walldorf, Germany) at −25°C. The sections were placed on 0.01% poly-L-lysine (Sigma) coated slides and kept in slide boxes at −20°C before immunofluorescent staining.

Cryosections of the gills were rinsed with phosphate-buffered saline (PBS) and then incubated in 5% BSA and 2% Tween 20 in PBS for 30 min. For double staining, the cryosections were then washed with PBS and incubated with the polyclonal anti-NKA antibody (#11) diluted in PBS overnight at 4°C. After incubation, the cryosections were washed several times with PBS, exposed to the secondary antibody (Alexa-flour 546 goat anti-rabbit antibody) at room temperature for 2 h, and then washed with PBS again. After the first staining, the cryosections were incubated with PBS-diluted monoclonal anti-NKCC (T4) antibodies, and then incubated for 2 h at room temperature. Subsequently, the cryosections were washed with PBS several times, followed by exposure to the secondary antibody (Alexa-flour 488 goat anti-mouse antibody) at room temperature for 2 h and then washed with PBS several times again. Finally, the double-immunostained cryosections were stained with a fluorescent dye, 4, 6-diamidino-2-phenylindole (DAPI, 1: 10,000 dilution in PBS; Sigma) at room temperature for 30 min and then washed with PBS several times. The sections were then covered by a coverslip with clearmount™ mounting solution (Zymed) and observed with a fluorescent microscope (BX50, Olympus). Micrographs were collected with a digital camera (Nikon COOLPIX 5000).

Statistical analysis

Values were compared using a one-way analysis of variance (ANOVA) followed by Tukey's pairwise method), and $P < 0.05$ was set as the significance level. Values were expressed as the mean ± S.E.M. (the standard error of the mean) unless stated otherwise.

Results

Survival rates after transfer from FW to SW and vice versa

No *M. argenteus* died after transfer from FW to SW or vice versa. The survival rates of both transfer groups, with 20 individuals each, were 100% in 7 days after being transferred. Thus, this species tolerated both the hyperosmotic and hyposmotic challenges to which they were subjected in this study.

Plasma analysis and muscle water content

According to our results (Table 1), there was no significant difference in plasma osmolality or plasma Na^+ and Cl^- concentrations among FW-, BW-, and SW-acclimated individuals. Additionally, the muscle water content of the FW group was slightly, but not significantly lower than that of the BW and SW groups (Table 1).

Ultrastructures of apical surfaces of mitochondrion-rich (MR) cells

Scanning electron micrographs showed that the epithelial MR cells were distributed close to the interlamellar regions of gill filaments of the FW-, BW-, and SW-acclimated *M. argenteus* (Fig. 1). Furthermore, the branchial MR cells from all groups exhibited microvilli on their apical openings (Fig. 1). The smallest and largest apical openings of the MR cells were found in the BW and FW fish, respectively (Fig. 1).

Numbers and sizes of Na^+, K^+-ATPase immunoreactive (NKA-IR) cells

The NKA-IR cells (i.e., MR cells) were mainly distributed in the epithelia of the interlamellar regions of the filaments. In the FW-acclimated *M. argenteus*, some NKA-IR cells were also found in the basal regions of the lamellae (Fig. 2). The quantified average number of NKA-IR cells in the filaments and lamellae of the FW group was significantly higher (approximately 1.8-fold) than that of the BW and SW groups (Fig. 3a). The smallest sized NKA-IR cells were found in the BW group, and these were significantly smaller than in FW and SW individuals (2.0- and 1.8-fold, respectively) (Fig. 3b).

Protein abundance and enzyme activity of NKA

Immunoblots of the NKA α-subunit probed with the α5 antibody indicated single immunoreactive bands of 100 kDa in the gills of all acclimated groups (Fig. 4a), and the intensities of the immunoreactive bands of the NKA α-subunit in the gills of different salinity groups revealed that the level in FW-acclimated *M. argenteus* was significantly higher (approximately 2.5-fold) than in the other groups, but there was no significant difference between the BW and SW groups (Fig. 4b).

The highest activity of branchial NKA was found in the FW-acclimated fish. The levels of the FW fish were significantly higher (approximately 2.0-fold)

Table 1 Plasma osmolality, Na^+, Cl^- concentrations, and muscle water content of *M. argenteus* acclimated to freshwater (FW), brackish water (BW), and seawater (SW)

Environments	FW	BW	SW
Plasma osmolality (mosmol kg^{-1})	340.88 ± 2.35	343.88 ± 6.77	356.75 ± 8.75
Plasma Cl^- concentration (mmol kg^{-1})	149.00 ± 7.82	160.97 ± 7.92	157 ± 463.38
Plasma Na^+ concentration (mmol kg^{-1})	136.23 ± 2.97	133.33 ± 7.18	145.87 ± 4.87
Muscle water contents (%)	68.39 ± 0.71	72.52 ± 2.01	71.35 ± 0.72

There is no significant difference. The data were analyzed with Tukey's multiple comparison test following one-way ANOVA ($P < 0.05$, $N = 8$). Values are means ± S.E.M

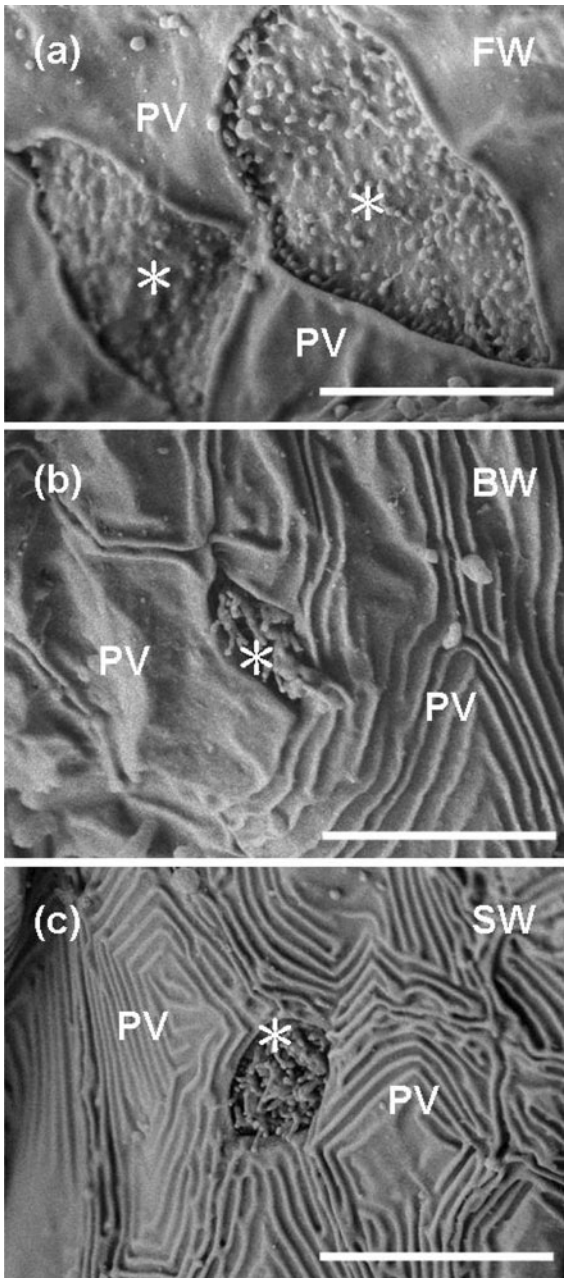

Fig. 1 Scanning electron micrographs showing the apical surface of mitochondrion-rich (MR) cells on the epithelia of the interlamellar regions in gill filaments of FW- (**a**), BW- (**b**), and SW-acclimated *M. argenteus* (**c**). Branchial MR cells (*star*) from all groups exhibited microvilli on the apical area. *Bar* = 5 μm. *PV* pavement cell, *FW* freshwater, *BW* brackish water, *SW* seawater

than those of the BW and SW groups, but no significant difference was found between the other two salinity groups (Fig. 5).

Na^+, K^+, $2Cl^-$ cotransporter 1 (NKCC1) protein expression

The immunoblots of NKCC1 in the *M. argenteus* gills probed with the T4 antibody indicated immunoreactive bands at 100 kDa in all groups (Fig. 6a). There were additional immunoreactive bands at 140 kDa in the BW and SW groups. Quantification of these two immunoreactive bands from the gill lysates of the different salinity groups revealed that the lowest levels of NKCC1 were found in the FW group, whereas levels in BW and SW individuals were approximately 2.4- and 4.5-fold higher, respectively (Fig. 7b). The protein levels of the SW fish were significantly higher (approximately 1.9-fold) than those of the BW fish. The relative amounts of branchial NKCC1 were salinity-dependent and increased with the level of environmental salinity.

Distribution of branchial NKCC1 protein

Immunofluorescent double staining was performed in the different groups using anti-NKA (#11) and anti-NKCC (T4) antibodies. The merged images of selected interlamellar regions of the filament epithelia of the FW, BW, and SW fish showed that NKCC1 immunoreactive (IR) signals were colocalized to the basolateral membrane of NKA-IR cells (Fig. 7). However, in FW individuals, some NKA-IR cells did not exhibit simultaneous NKCC1-IR signals (Fig. 7d). Additionally, micrographs of DAPI staining were used to distinguish the nuclei of the NKA-IR cells in the sections.

Discussion

The survival rates of euryhaline teleosts following direct or gradual transfer between different salinity environments are generally observed to determine their salinity tolerance ability (Hiroi and McCormick 2007; Kang et al. 2010). Hence, salinity tolerance in the juvenile silver moony (*Monodactylus argenteus*) was observed in this study to evaluate the euryhalinity of this species as a candidate for studying osmoregulatory mechanisms. The observed survival rates indicated that this marine euryhaline species exhibits great salinity tolerance, similar to other marine species, including milkfish (Lin et al. 2003),

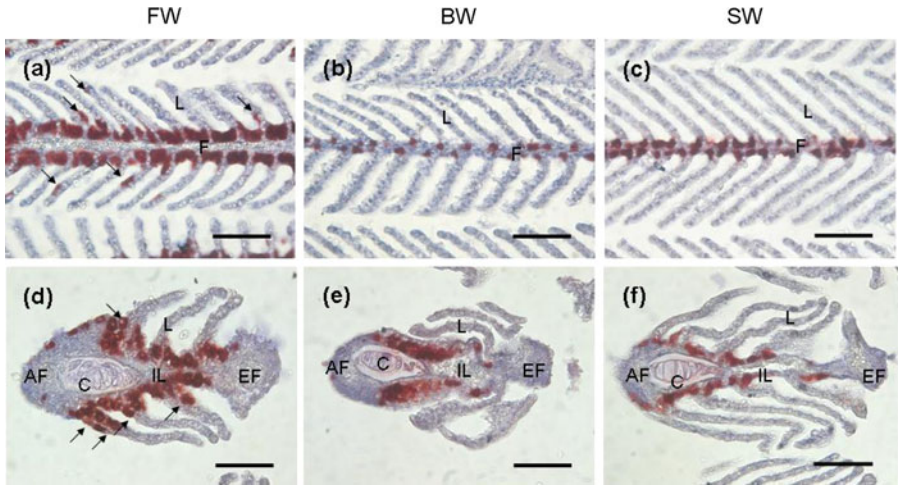

Fig. 2 Immunohistochemical staining of the Na^+, K^+-ATPase (NKA) α-subunit in longitudinal sections (**a**, **b**, **c**) and cross-sections (**d**, **e**, **f**) of gills of *M. argenteus* acclimated to FW (**a**, **d**), BW (**b**, **e**), or SW (**c**, **f**). The NKA immunoreactive (NKA-IR) cells (*red*) were mainly distributed in the epithelium of the interlamellar regions of the filaments. Only the FW-acclimated *M. argenteus* were found to have NKA-IR cells on their lamellae (*arrows*). *Bar* = 50 μm. *AF* afferent region, *BW* brackish water, *C* cartilage, *EF* efferent region, *FW* freshwater, *IL* interlamellar region, *L* lamellae, *SW* seawater

spotted green pufferfish (Lin et al. 2004b), and brackish medaka (Inoue and Takei 2002, 2003). In addition, the plasma osmolality and Na^+ and Cl^- concentrations, as well as the muscle water content, of the silver moony did not change with environmental salinity (Table 1). Similar patterns for these parameters have been found in other euryhaline teleosts, including gilthead seabream (Mancera et al. 1993), mullet (Ciccotti et al. 1994), turbot (Gaumet et al. 1995), emperor angelfish (Woo and Chung 1995), seabass (Jensen et al. 1998), black seabream (Kelly et al. 1999), milkfish (Lin et al. 2004a; Tang et al. 2009), brackish medaka (Kang et al. 2008), and spotted green pufferfish (Lin et al. 2004b). Our findings revealed that *M. argenteus* has a great osmoregulatory capacity to absorb and secrete ions for maintaining plasma homeostasis when exposed to environments of different salinities.

The SEM observations showed that the apical areas of the MR cells of FW *M. argenteus* were bigger than in the SW fish (Fig. 1), similar to the patterns found in killifish, mullet, tilapia, seabass, and seabream (Hossler et al. 1985; Lee et al. 1996; Chang et al. 2002; Katoh and Kaneko 2003). In the other euryhaline species, the apical surfaces of the MR cells were flat type in FW and hole type in SW treatments (Hossler et al. 1985; Lee et al. 1996; Chang et al. 2002; Katoh and Kaneko 2003; Kaneko et al. 2008). Furthermore, the apical membranes of the MR cells in FW individuals usually exhibited microvillus structures (Hossler et al. 1985; Lee et al. 1996; Chang et al. 2002; Katoh and Kaneko 2003). However, flat-type MR cells with microvilli were found not only in FW-acclimated *M. argenteus* but also in the BW and SW fish in this study (Fig. 1). Microvillus-containing flat-type MR cells have also been found in the yellowtail (*Seriola quinqueradiata,* Doi et al. 1981). It has been suggested that these marine teleosts expand the surface area of the apical membrane of their MR cells with microvilli to increase the efficiency of ion secretion in SW.

Previous studies indicated that the MR cells express the highest levels of Na^+, K^+-ATPase (NKA) in teleostean gills (Karnaky et al. 1976; Marshall and Bryson 1998; Hirose et al. 2003; Lin et al. 2004a; Hwang and Lee 2007). The cross-sections of the gill filaments showed that the NKA immunoreactive (NKA-IR) cells of *M. argenteus* that acclimated to FW, BW, or SW were distributed mainly in the interlamellar region near the afferent side of the filament but rarely appeared on the afferent region of the filament (Fig. 2), similar to the distribution of MR cells in the gills of rainbow trout (Olson and Fromm 1973) and milkfish (Lin et al. 2003). In addition, NKA-IR cells were also found on the lamellar epithelium in FW-adapted silver moony gills, confirming the results of Lin and Sung (2003).

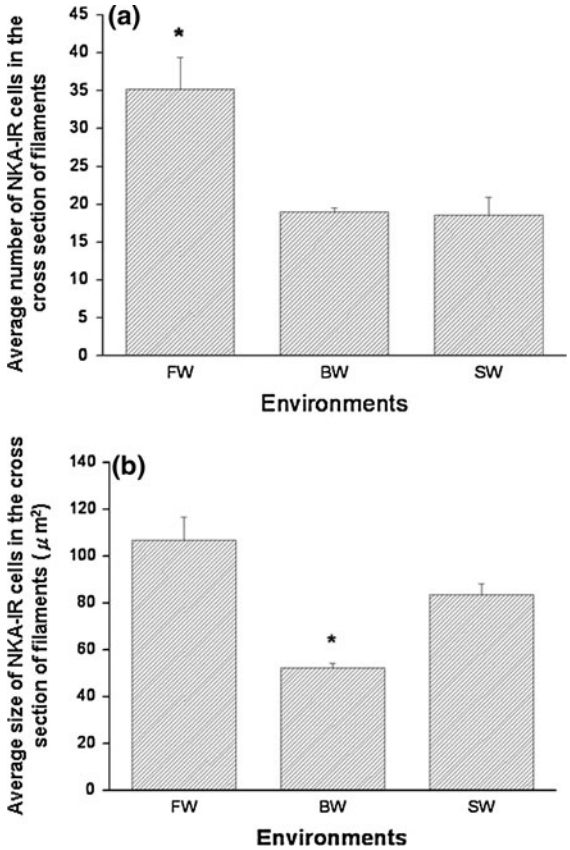

Fig. 3 **a** Quantified average numbers of NKA-IR cells in cross-sections of filaments from the gills of *M. argenteus* acclimated to FW, BW, and SW. The average number of NKA-IR cells in the filaments and lamellae of the FW group was significantly higher than in the BW and SW groups. **b** Quantified average sizes of NKA-IR cells in cross-sections of filaments from the gills of *M. argenteus* acclimated to FW, BW, and SW. The average size of NKA-IR cells in the filaments and lamellae of the BW group was significantly smaller than in the FW and SW groups. The *asterisks* indicate significant differences ($P < 0.05$) using Tukey's multiple comparison test following one-way ANOVA. Values are means ± S.E.M ($n = 5$ for all groups). *FW* freshwater, *BW* brackish water, *SW* seawater

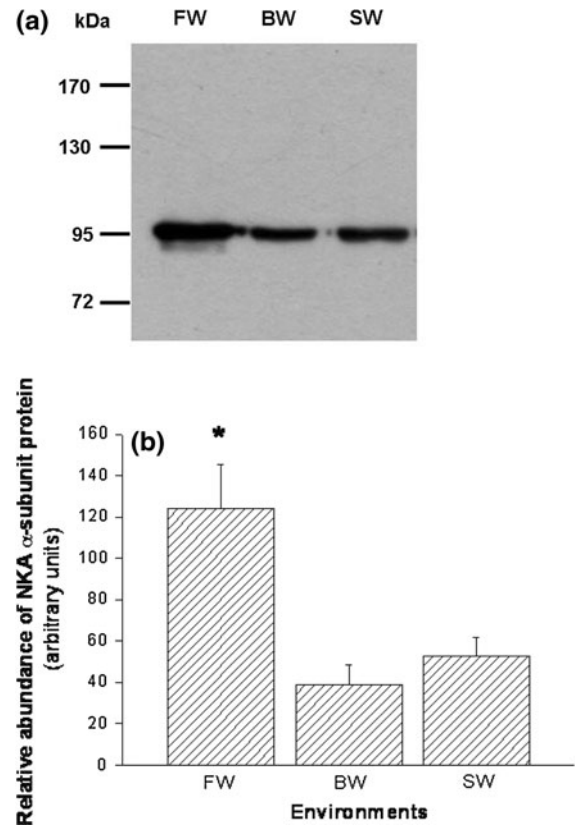

Fig. 4 Expression of NKA α-subunit protein in gills of *M. argenteus* acclimated to FW, BW, or SW. **a** Immunoblots of *M. argenteus* gills probed with the α5 antibody indicated single immunoreactive bands at 100 kDa in all environmental groups. **b** The intensities of the immunoreactive bands of the NKA α-subunit in gills of different salinity groups ($n = 4$ for all groups) revealed that FW-acclimated *M. argenteus* was significantly higher than the other groups. The *asterisk* indicated a significant difference ($P < 0.05$) using Tukey's multiple comparison test following one-way ANOVA. Values are means ± S.E.M. *FW* freshwater, *BW* brackish water, *SW* seawater

Lamellar MR cells in the gills of FW stenohaline fish and FW-adapted euryhaline fish participated in ion uptake when acclimated to the hyposmotic environments (Lee et al. 1996; Lin and Sung 2003; Sakamoto et al. 2001, Tang et al. 2008). The number and size of MR cells in some euryhaline teleosts change with external salinities in some cases (Hwang and Lee 2007). The highest number and density of MR cells in the black seabream (Kelly et al. 1999), seabass (Versamos et al. 2002), milkfish (Lin et al. 2003, 2006), and brackish medaka (Kang et al. 2008) were found in hyposmotic environments. The changing pattern of the number of NKA-IR cells observed in *M. argenteus* conformed to what has been observed in other marine species (Fig. 3a). Meanwhile, the smallest size of NKA-IR cells was found in BW-acclimated *M. argenteus* (Fig. 3b), similar to observations for the brackish medaka (Kang et al. 2008). Taken together, these results indicate that in low salinity environments, the NKA-IR cells of *M. argenteus* increase in size and number to carry out osmoregulatory roles.

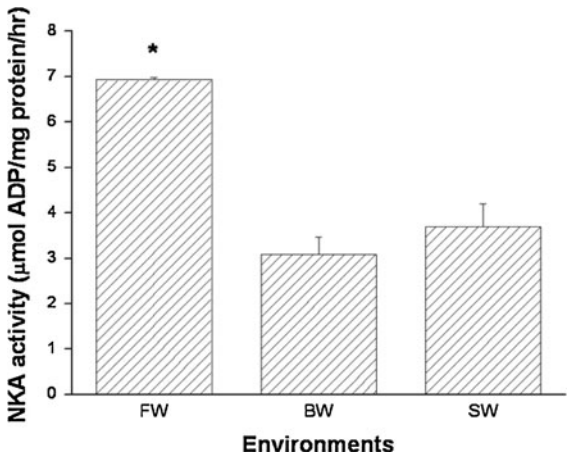

Fig. 5 Gill NKA activity of *M. argenteus* acclimated to FW, BW, or SW ($n = 10$ for all groups). The activity of FW *M. argenteus* was significantly higher than the other groups (*asterisk*). The data were analyzed with Tukey's multiple comparison test following one-way ANOVA. Values are means ± S.E.M. *FW* freshwater, *BW* brackish water, *SW* seawater

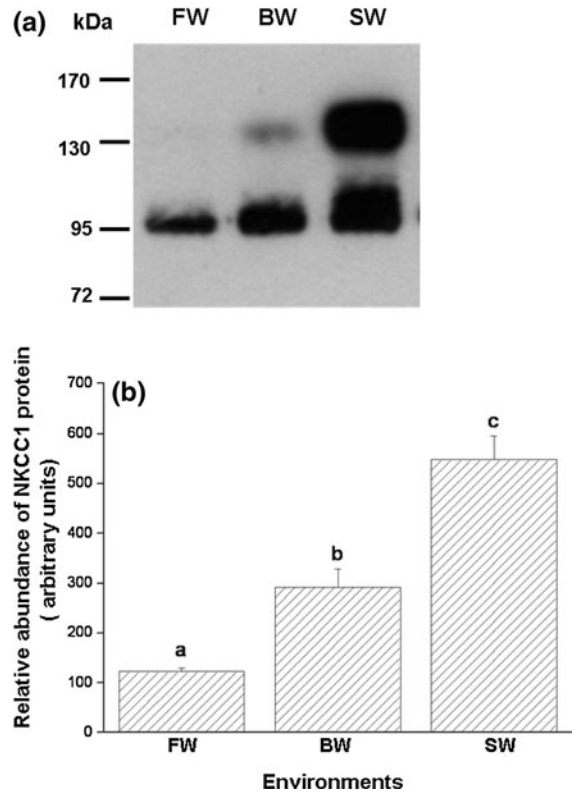

Fig. 6 Expression of Na^+, K^+, $2Cl^-$ cotransporter 1 (NKCC1) protein in gills of *M. argenteus* acclimated to FW, BW, or SW. **a** Immunoblots of *M. argenteus* gills probed with the T4 antibody indicated two immunoreactive bands, one of 100 kDa in all environmental groups and another band at 140 kDa in the BW and SW groups. **b** The quantified intensities of the two immunoreactive bands in gills of different salinity groups ($n = 4$ for all groups) revealed that levels in SW-acclimated *M. argenteus* were significantly higher than the other groups. Different letters indicated a significant difference ($P < 0.05$) using Tukey's multiple comparison test following one-way ANOVA. Values are means ± S.E.M. *FW* freshwater, *BW* brackish water, *SW* seawater

Euryhaline teleosts generally exhibit the lowest branchial NKA activities in environments with salinities similar to their natural habitats (Hwang and Lee 2007). Furthermore, higher NKA α-subunit protein abundance in the gills of the euryhaline teleosts always accompanies increased branchial NKA activity in response to environmental salinities different than their natural habitats (Tipsmark et al. 2002; Lee et al. 2003; Lin et al. 2004a, b; Kang et al. 2008). The results of this study revealed that the lowest NKA α-subunit protein abundance and NKA activity were exhibited in the BW- and SW-acclimated *M. argenteus* (Figs. 4, 5). The pattern of NKA expression was similar to that found in other euryhaline teleosts residing BW and SW, including sea bass (Jensen et al. 1998), milkfish (Lee et al. 2003), and brackish medaka (Kang et al. 2008). Changes in NKA protein abundance and NKA-IR cell profiles might contribute to alterations in NKA activity for the purpose of ionoregulation (Dang et al. 2000; Lin et al. 2003; Kang et al. 2008). In addition, the pattern of changing numbers of MR cells was similar to that of the protein abundance and activity of NKA in the gills of *M. argenteus*, as described above. Thus, these results suggested that the increased number of NKA-IR cells provided expanded tubular systems where gill NKA was located and led to an increase in NKA protein abundance and activity. Langdon (1987) reported that juvenile fish that maintained internal homeostasis with the lowest NKA activity had more energy available for growth. Therefore, the present study suggested that BW-acclimated *M. argenteus* might cost the lowest energy for ionoregulation of gills. The optimal environmental salinity in which to raise juvenile *M. argenteus* was found to be 15‰ ($[Na^+]$ 156.11 ± 4.50 mM; $[K^+]$ 5.72 ± 0.06 mM; $[Ca^{2+}]$ 9.29 ± 0.28 mM; $[Mg^{2+}]$ 30.34 ± 1.29 mM; $[Cl^-]$ 270.60 ± 12.07 mM).

The distribution and expression of branchial Na^+, K^+, $2Cl^-$ cotransporter 1 (NKCC1) protein have been

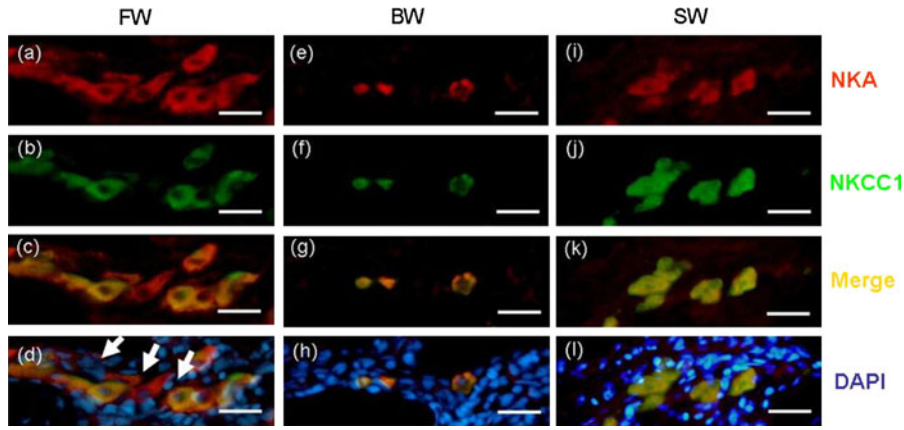

Fig. 7 Fluorescent micrographs of cross-sections of *M. argenteus* gills acclimated to FW, BW, and SW. Immunofluorescent double staining was performed in the different groups using anti-NKA (polyclonal antibody; *red*; **a**; **e**; **i**) and anti-NKCC (monoclonal antibody (T4); *green*; **b**; **f**; **j**) antibodies. Micrographs of DAPI staining (**d**, **h**, **l**) were used to check the structure of these samples. Merged images (**c**, **g**, **k**) of randomly selected epithelial regions in filaments revealed that NKCC1 colocalized to the basolateral membrane of NKA-IR cells in the FW, BW, and SW fish. The *arrows* indicate NKA-IR cells that had no NKCC1-IR signal. *Bar* = 10 μm. *FW* freshwater, *BW* brackish water, *SW* seawater

detected using a monoclonal anti-human NKCC1 antibody (T4) in euryhaline teleosts in a number of recent studies (Pelis et al. 2001; Wu et al. 2003; Hiroi and McCormick 2007; Katoh et al. 2008, Tang and Lee 2007; Kang et al. 2010). In this study, we found that the molecular weights of the immunoreactive bands detected from gill lysates of *M. argenteus* were from 100 to 140 kDa (Fig. 6a), which is similar to what was found for smear or poly bands on immunoblots using the same antibody for pufferfish (Tang and Lee 2007), salmon (Pelis et al. 2001; Hiroi and McCormick 2007), and tilapia (Hiroi et al. 2008). However, the FW group exhibited only the 100-kDa immunoreactive band. According to the peptide sequences of NKCC1 in other fish, two potential N-linked glycosylation sites are predicted. Different degrees of glycosylation might lead to variable molecular weights of NKCC1 in the immunoblots (Tipsmark et al. 2002; Wu et al. 2003, Kang et al. 2010). Therefore, our results suggested that the form of NKCC1 found in the FW-acclimated *M. argenteus*, without glycosylation, was not an active form. The quantification of these two immunoreactive bands revealed that the abundance of branchial NKCC1 was salinity-dependent in the gills of *M. argenteus* (Fig. 6b), similar to what has been found in many other euryhaline species, including eel (Tse et al. 2006), flounder (Tipsmark et al. 2008a, b), goby (Chew et al. 2009), killifish (Scott et al. 2004), pufferfish (Tang and Lee. 2007), salmon (Pelis et al. 2001; Tipsmark et al. 2002; Hiroi and McCormick 2007; Nilsen et al. 2007), sea bass (Lorin-Nebel et al. 2006), striped bass (Tipsmark et al. 2004), sturgeon (Sardella and Kültz 2009), tilapia (Wu et al. 2003; Tipsmark et al. 2008a), and brackish medaka (Kang et al. 2010). Thus, the salinity-dependent expression of branchial NKCC1 has been found to be conserved in euryhaline teleosts from different niches of their phylogenic tree.

The colocalization of NKCC1 and NKA in the gills of BW- and SW-acclimated *M. argenteus* (Fig. 7) revealed that NKCC1 was located at the basolateral membrane of MR cells. The distribution of NKCC1 conformed to the currently accepted model of Cl^- secretion via branchial MR cells in SW fish (Pelis et al. 2001; Wu et al. 2003; Evans et al. 2005; Hiroi and McCormick 2007; Katoh et al. 2008). Similar results were found in the FW-acclimated silver moony and in other hyposmotic media-acclimated marine fish, including goby, pufferfish, and sturgeon (McCormick et al. 2003; Prodocimo and Freire 2006; Sardella and Kültz 2009). The patterns of these marine teleosts, however, violated the model of the absorptive Na^+, Cl^-, cotransporter (NCC) protein (apical T4 signals) in tilapia and zebrafish, in response to environments with low [Cl^-] (Hiroi et al. 2008; Wang et al. 2009). The pattern also suggested that marine euryhaline fish exhibited another Cl^--

absorbing mechanism without a role of the NCC protein when exposed to hyposmotic environments. However, Kang et al. (2010) reported that when SW-acclimated brackish medaka were exposed to FW, the levels of branchial NKCC1 retained were correlated with their hyposmoregulatory endurance. Our immunoblotting and immunostaining results suggested that FW-acclimated *M. argenteus* expressed low level of a non-active form of NKCC1 on the basolateral membrane of some branchial MR cells to provide greater hyposmoregulatory endurance for salinity tolerance upon hyperosmotic challenges.

In summary, the juvenile silver moony, which resides in river mouths or estuaries, where salinity fluctuates dramatically, exhibit great salinity tolerance and maintained plasma homeostasis within limited ranges through an efficient adaptive osmoregulatory mechanism. When *M. argenteus* was acclimated to FW, MR cells with a larger apical surface were observed to proliferate in the gill filaments and lamellae for absorbing ions; NKA activity was elevated to supply a greater driving force for ion transport, and low level of NKCC1 expression was maintained for conferring hyposmoregulatory endurance. The present study illustrated a number of the osmoregulatory mechanisms of this easy- and economic-to-rear marine teleost with euryhaline capacity and proved the silver moony to be a good experimental animal for future ecophysiological studies.

Acknowledgments This study was supported by a grant to T.H.L. (NSC 95-2311-B-005-040-MY3) and an Undergraduate Student Research Project to F.C.L. (NSC98-2815-C-005-084 - B) from the National Science Council of Taiwan. The monoclonal antibody T4 and α5 was purchased from the Developmental Studies Hybridoma Bank (DSHB) maintained by the Department of Pharmacology and Molecular Sciences, John Hopkins University School of Medicine, Baltimore, MD 2120521205, and the Department of Biological Sciences, University of Iowa, Iowa City, IA 52242, under Contract N01-HD-6-2915, NICHD, USA.

References

Chang IC, Lee TH, Wu HC, Hwang PP (2002) Effects of environmental Cl^- levels on Cl^- uptake and mitochondria-rich cell morphology in gills of the stenohaline goldfish, *Carassius auratus*. Zool Stud 46:236–243

Chew SF, Tng YYM, Wee NLJ, Wilson JM, Ip YK (2009) Nitrogen metabolism and branchial osmoregulatory acclimation in the juvenile marble goby, *Oxyeleotris marmorata*, exposed to seawater. Comp Biochem Physiol 154A:360–369

Ciccotti E, Marino G, Pucci P, Cataldi E, Cataudella S (1994) Acclimation trial of *Mugil cephalus* juveniles to freshwater: morphological and biochemical aspects. Environ Biol Fish 43:163–170

Dang Z, Lock RAC, Flik G, Bonga SEW (2000) Na^+/K^+-ATPase immunoreactivity in branchial chloride cells of *Oreochromis mossambicus* exposed to copper. J Exp Biol 203:379–387

Doi A, Hatase O, Shimada M, Murakami TH, Okaichi T (1981) Ultrastructural changes in gill epithelia of a yellowtail, *Seriola quinqueradiata*, exposed to sea bloom. Cell Str Func 6:375–383

Evans DH (2008) Teleost fish osmoregulation: what have we learned since August Krogh, Homer Smith, and Ancel Keys. Am J Physiol 295:R704–R713

Evans DH, Piermarini PM, Choe KP (2005) The multifunctional fish gill: dominant site of gas exchange, osmoregulation, acid-base regulation, and excretion of nitrogenous waste. Physiol Rev 85:97–177

Fernhead EA, Fabian BL (1971) The ultrastructure of the gill of *Monodactylus argenteus* (an euryhaline teleost fish) with particular reference to morphological changes associated with changes in salinity. South Afr Assoc Mar Biol Res Oceanogr Res Inst Invest Rep 26:39

Franson MAH (1985) Standard methods for the examination of water and waste water, 16th edn. American Public Health Association, Washington

Gaumet F, Boeuf G, Severe A, Le Roux A, Mayer-Gostan N (1995) Effects of salinity on the ionic balance and growth of juvenile turbot. J Fish Biol 47:865–876

Hiroi J, McCormick SD (2007) Variation in salinity tolerance, gill Na^+/K^+-ATPase, $Na^+/K^+/2Cl^-$ cotransporter and mitochondria-rich cell distribution in three salmonids *Salvelinus namaycush*, *Salvelinus fontinalis* and *Salmo salar*. J Exp Biol 210:1015–1024

Hiroi J, Yasumasu S, McCormick SD, Hwang PP, Kaneko T (2008) Evidence for an apical Na–Cl cotransporter involved in ion uptake in a teleost fish. J Exp Biol 211:2584–2599

Hirose S, Kaneko T, Naito N, Takei Y (2003) Molecular biology of major components of chloride cells. Comp Biochem Physiol 136B:593–620

Hossler FE, Musil G, Karnaky KJ, Epstein FH (1985) Surface ultrastructure of the gill arch of the killifish, *Fundulus heteroclitus*, from seawater and fresh water, with special reference to the morphology of apical crypts of chloride cells. J Morphol 185:377–386

Hwang PP, Lee TH (2007) New insights into fish ion regulation and mitochondrion-rich cells. Comp Biochem Physiol 148A:479–497

Inokuchi M, Hiroi J, Watanabe S, Hwang PP, Kaneko T (2009) Morphological and functional classification of ion-absorbing mitochondria-rich cells in the gills of Mozambique tilapia. J Exp Biol 212:1003–1010

Inoue K, Takei Y (2002) Diverse adaptability in *Oryzias* species to high environmental salinity. Zool Sci 19:727–734

Inoue K, Takei Y (2003) Asian medaka fishes offer new models for studying mechanisms of seawater adaptation. Comp Biochem Physiol 136B:635–645

Jensen MK, Madsen SS, Kristiansen K (1998) Osmoregulation and salinity effects on the expression and activity of Na^+/K^+-ATPase in the gills of European sea bass, *Dicentrarchus labrax* (L.). J Exp Zool 282:290–300

Kaneko T, Watanabe S, Lee KM (2008) Functional morphology of mitochondrion-rich cells in euryhaline and stenohaline teleosts. Aqua BioSci Monogr 1:1–62

Kang CK, Tsai SC, Lee TH, Hwang PP (2008) Differential expression of branchial Na^+/K^+-ATPase of two medaka species, *Oryzias latipe*s and *Oryzias dancena*, with different salinity tolerances acclimated to fresh water, brackish water and seawater. Comp Biochem Physiol 151A:566–575

Kang CK, Tsai HJ, Liu CC, Lee TH, Hwang PP (2010) Salinity-dependent expression of a Na^+, K^+, $2Cl^-$ cotransporter in gills of the brackish medaka *Oryzias dancena*: a molecular correlate for hyposmoregulatory endurance. Comp Biochem Physiol 157A:7–18

Karnaky KJ, Kinter LB, Kinter WB, Stirling CE (1976) Teleost chloride cell II. Autoradiographic localization of gill Na, K-ATPase in killifish *Fundulus* heteroclitus adapted to low and high salinity environments. J Cell Biol 70:157–177

Katoh F, Kaneko T (2003) Short-term transformation and long-term replacement of branchial chloride cells in killifish transferred from seawater to freshwater, revealed by morph functional observations and a newly established 'time-differential double fluorescent staining' technique. J Exp Biol 206:4113–4123

Katoh F, Cozzi RRF, Marshall WS, Goss GG (2008) Distinct $Na^+/K^+/2Cl^-$ cotransporter localization in kidneys and gills of two euryhaline species, rainbow trout and killifish. Cell Tissue Res 334:265–281

Kelly SP, Chow INK, Woo NYS (1999) Haloplasticity of black seabream (*Mylio macrocephalus*): hypersaline to freshwater acclimation. J Exp Zool 283:226–241

Langdon JS (1987) Active osmoregulation in the Australian bass, *Macquaria novemaculata* (Steindachner), and the golden perch, *Macquaria ambigua* (Richardson) (Percichthyidae). Aust J Mar Freshw Res 38:771–776

Lee TH, Hwang PP, Lin HC, Huang FL (1996) Mitochondria-rich cells in the branchial epithelium of the teleost, *Oreochromis mossambicus*, acclimated to various hypotonic environments. Fish Physiol Biochem 15:513–523

Lee TH, Feng SH, Lin CH, Hwang YH, Huang CL, Hwang PP (2003) Ambient salinity modulates the expression of sodium pumps in branchial mitochondria-rich cells of Mozambique tilapia, *Oreochromis mossambicus*. Zool Sci 20:29–36

Lin HC, Sung WT (2003) The distribution of mitochondria-rich cells in the gills of air-breathing fishes. Physiol Biochem Zool 76:215–228

Lin YM, Chen CN, Lee TH (2003) The expression of gill Na^+/K^+-ATPase in milkfish, *Chanos chanos*, acclimated to seawater, brackish water and fresh water. Comp Biochem Physiol 135A:489–497

Lin CH, Huang CL, Yang CH, Lee TH, Hwang PP (2004a) Time-course changes in the expression of Na^+/K^+-ATPase and the morphometry of mitochondrion-rich cells in gills of euryhaline tilapia (*Oreochromis mossambicus*) during freshwater acclimation. J Exp Zool 301A:85–96

Lin CH, Tsai RS, Lee TH (2004b) Expression and distribution of Na^+/K^+-ATPase in gills and kidneys of the green spotted pufferfish, Tetraodon nigroviridis, in response to salinity challenge. Comp Biochem Physiol 138A:287–295

Lin YM, Chen CN, Yoshinaga T, Tsai SC, Shen ID, Lee TH (2006) Short-term effects of hyposmotic shock on Na^+/K^+-ATPase expression in gills of the euryhaline milkfish, *Chanos chanos*. Comp Biochem Physiol 143A:406–415

Linnaeus C (1758) Systema naturae per regna tria naturae, secundum classes, ordinus, genera, species, cum characteribus, differentiis, synonymis, locis. Tomus I. Editio decima, reformata. Impensis Direct. Laurentii Salvii, Holmiae. 824 p

Lorin-Nebel C, Boulot V, Bodinier C, Charmantier G (2006) The $Na^+/K^+/2Cl^-$ cotransporter in the sea bass *Dicentrarchus labrax* ontogeny: involvement in osmoregulation. J Exp Biol 209:4908–4922

Lytle C, Xu JC, Biemesderfer D, Forbush B III (1995) Distribution and diversity of Na–K–Cl cotransport proteins: a study with monoclonal antibodies. Am J Physiol 269:C1496–C1505

Mancera JM, Perez-Figares JM, Fernandez-Llebrez P (1993) Osmoregulatory responses to abrupt salinity changes in the euryhaline gilthead sea bream (*Sparus aurata L*). Comp Biochem Physiol 106A:245–250

Marshall WS (2002) Na^+, Cl^-, Ca^{2+} and Zn^{2+} transport by fish gills: retrospective review prospective synthesis. J Exp Zool 293:264–283

Marshall WS, Bryson SE (1998) Transport mechanisms of seawater teleost chloride cells: an inclusive model of a multifunctional cell. Comp Biochem Physiol 119A:97–106

McCormick SD (1993) Methods for nonlethal gill biopsy and measurement of Na^+, K^+-ATPase activity. Can J Fish Aquat Sci 50:656–658

McCormick SD, Sundell K, Bjornsson BT, Brown CL, Hiroi J (2003) Influence of salinity on the localization of Na^+/K^+-ATPase, $Na^+/K^+/2Cl^-$ cotransporter (NKCC) and CFTR anion channel in chloride cells of the Hawaiian goby (*Stenogobius hawaiiensis*). J Exp Biol 206:4575–4583

Nilsen TO, Ebbesson LO, Madsen SS, McCormick SD, Andersson E, Bjornsson BT, Prunet P, Stefansson SO (2007) Differential expression of gill Na^+, K^+-ATPase α- and β-subunits, Na^+, K^+, $2Cl^-$cotransporter and CFTR anion channel in juvenile anadromous and landlocked Atlantic salmon *Salmo salar*. J Exp Biol 210:2885–2896

Olson KR, Fromm PO (1973) A scanning electron microscope study of secondary lamellae and chloride cells of rainbow trout (*Salmo gairdneri*). Z Zellforsch 143:439–449

Pelis RM, Zydlewski J, McCormick SD (2001) Gill Na^+-K^+-$2Cl^-$ cotransporter abundance and location in Atlantic salmon: effects of seawater and smolting. Am J Physiol 280:R1844–R1852

Prodocimo V, Freire CA (2006) The Na^+, K^+, $2Cl^-$ cotransporter of estuarine pufferfishes (*Sphoeroides testudineus* and *S. greeleyi*) in hypo- and hyper-regulation of plasma osmolality. Comp Biochem Physiol 143C:347–355

Sakamoto T, Uchida K, Yokota S (2001) Regulation of the ion-transporting mitochondrion-rich cell during adaptation of teleosts fishes to different salinities. Zool Sci 18:1163–1174

Sardella BA, Kültz D (2009) Osmo- and ionoregulatory responses of green sturgeon (*Acipenser medirostris*) to salinity acclimation. J Comp Physiol 179B:383–390

Scott GR, Richards JG, Forbush B, Isenring P, Schulte PM (2004) Changes in gene expression in gills of the euryhaline killifish *Fundulus heteroclitus* after abrupt salinity transfer. Am J Physiol 287:C300–C309

Shao KT (Eds.) (2009) Taiwan fish database. WWW Web electronic publication. http://fishdb.sinica.edu.tw, version (01/2009)

Starremans PG, Kersten FF, Van Den Heuvel LP, Knoers NV, Bindels RJ (2003) Dimeric architecture of the human bumetanide-sensitive Na-K-Cl Co-transporter. J Am Soc Nephrol 14:3039–3046

Tang CH, Lee TH (2007) The effect of environmental salinity on the protein expression of Na^+/K^+-ATPase, $Na^+/K^+/2Cl^-$ cotransporter, cystic fibrosis transmembrane conductance regulator, anion exchanger 1, and chloride channel 3 in gills of a euryhaline teleost, *Tetraodon nigroviridis*. Comp Biochem Physiol 147A:521–528

Tang CH, Chang IC, Chen CH, Lee TH, Hwang PP (2008) Phenotypic changes of mitochondrion-rich cells and responses of Na^+/K^+-ATPase in gills of tilapia exposed to deionized water. Zool Sci 25:205–211

Tang CH, Tzeng CS, Hwang LY, Lee CH (2009) Constant muscle water content and renal HSP90 expression reflect osmotic homeostasis in euryhaline teleosts acclimated to different environmental salinities. Zool Stud 48:435–441

Tipsmark CK, Madsen SS, Seidelin M, Christensen AS, Cutler CP, Cramb G (2002) Dynamics of Na^+, K^+, $2Cl^-$ cotransporter and Na^+, K^+-ATPase expression in the branchial epithelium of brown trout (*Salmo trutta*) and Atlantic salmon (*Salmo salar*). J Exp Zool 293:106–118

Tipsmark CK, Madsen SS, Borski RJ (2004) Effect of salinity on expression of branchial ion transporters in striped bass (*Morone saxatilis*). J Exp Zool A 301:979–991

Tipsmark CK, Baltzegar DA, Ozden O, Grubb BJ, Borski RJ (2008a) Salinity regulates claudin mRNA and protein expression in the teleost gill. Am J Physiol 294:R1004–R1014

Tipsmark CK, Luckenbach JA, Madsen SS, Kiilerich P, Borski RJ (2008b) Osmoregulation and expression of ion transport proteins and putative claudins in the gill of southern flounder (*Paralichthys lethostigma*). Comp Biochem Physiol 150A:265–273

Tse WKF, Au DWT, Wong CKC (2006) Characterization of ion channel and transporter mRNA expressions in isolated gill chloride and pavement cells of seawater acclimating eels. Biochem Biophy Res Comm 346:1181–1190

Versamos S, Diaz JP, Charmantier G, Flik G, Blasco C, Connes R (2002) Branchial chloride cells in sea bass (*Dicentrarchus labrax*) adapted to fresh water, seawater, and doubly concentrated seawater. J Exp Zool 293:12–26

Wang YF, Tseng YC, Yan JJ, Hiroi J, Hwang PP (2009) Role of SLC12A10.2, a Na-Cl cotransporter-like protein, in a Cl uptake mechanism in zebrafish (*Danio rerio*). Am J Physiol 296:R1650–R1660

Woo NYS, Chung KC (1995) Tolerance of Pomacanthus imperator to hypoosmotic salinity: changes in body composition and hepatic enzyme activities. J Fish Biol 47:70–81

Wu YC, Lin LY, Lee TH (2003) Na, K, $2Cl^-$ cotransporter: a novel marker for identifying freshwater- and seawater-type mitochondria-rich cells in gills of euryhaline tilapia, *Oreochromis mossambicus*. Zool Stud 42:186–192